

# Experimental study of the time-resolved reflectivity of chromium film

Tengfei Wu (武腾飞), Changhe Zhou (周常河)\*, Enwen Dai (戴恩文), and Jin Xie (谢金)

*Information Optics Laboratory, State Key Laboratory of High Field Laser Physics,  
Shanghai Institute of Optics and Fine Mechanics,  
Chinese Academy of Sciences, Shanghai 201800, China*

\*E-mail: chazhou@mail.shcnc.ac.cn

Received September 16, 2008

The transient time-resolved reflectivity of chromium film is studied by femtosecond pump-probe technique with a 70-fs laser. Experimental results show that the reflectivity change increases with the power of the pump laser. The fast decrease of the reflectivity occurs between 0–200 fs which is mainly due to the electron-electron interaction. Subsequently, the slower recovery of the reflectivity between 200–900 fs is mainly due to the electron-phonon coupling process. The reflectivity after 900 fs rises little to a near-constant value for the thermal equilibrium of the system. The experimental results can be explained properly with numerical simulation of the two-temperature model. It is helpful for understanding of the electron ultrafast dynamics in chromium film.

OCIS codes: 320.2250, 320.7160, 310.6860.

doi: 10.3788/COL20090707.0653.

The femtosecond laser has been widely used in study of ultrafast dynamic process<sup>[1–5]</sup>. Because the pulse of femtosecond laser is shorter than the time scale of electron and phonon relaxation process in metals, a variety of femtosecond time-resolved measurement techniques were put forward for investigation of transient relaxation of hot electrons in metal film, such as optical pump-probe spectroscopy technique<sup>[5]</sup>, pump-probe high energy electron diffraction<sup>[6]</sup>, time-resolved linear and second-harmonic reflectivity measurements<sup>[7]</sup>, and femtosecond transient thermoreflectivity and transmissivity measurement technique<sup>[8–12]</sup>.

The electron transient relaxation process in noble metals with the relatively weak electron-phonon interaction was studied by time-resolved reflectivity technique<sup>[2,11,12]</sup>. The study of the transition metal (chromium) is interesting for the chromium has a strong electron-phonon coupling constant. Experiments about the interaction between the femtosecond laser and the chromium film was studied with double-pulse method<sup>[13,14]</sup>, where the laser power was above the laser damage threshold of the chromium film. A reversible dark-center diffraction of the chromium film was observed in the femtosecond pump-probe experiment, where the optical reflectivity of the pump area through chromium film was detected by using charge-coupled device (CCD)<sup>[15]</sup>. Electron excitation and relaxation in chromium were probed with the 20-fs laser<sup>[16]</sup>. However, the ultrafast electron dynamic process and the band structure of the chromium film were complex. The chromium film used in Ref. [16] is different from the chromium film on the mask in microelectronic industry. It is necessary to study the ultrafast electron dynamics of the chromium mask used in microelectronic industry.

In this letter, we report the experimental results of the femtosecond time-resolved reflectivity of chromium film using the femtosecond pump-probe technique for three different pump powers. Experimental results show that

the reflectivity change increases with the power of the pump laser. Numerical solutions of the two-temperature model (TTM) are compared with experimental results.

The experimental setup is shown in Fig. 1. A commercial 76-MHz Ti:sapphire laser oscillator (Coherent) was used in this experiments. The femtosecond pulse duration was 70 fs of full-width at half-maximum (FWHM). The average power and the center wavelength of the femtosecond laser were 550 mW and 800 nm, respectively. The pulses were measured by a home-made Dammann frequency-resolved optical grating (FROG) setup<sup>[17]</sup>. The femtosecond laser was divided into a probe beam and a pump beam. The delay time was controlled by the delay line. The polarization states of the probe beam and the pump beam were adjusted perpendicular to each other by a 1/2 wave plate for decreasing the coherent coupling effect. The ratio between the pump and probe beams was kept 100:1 by adjusting the attenuators. The optical spot radius of the pump and probe beams were 15 and 10  $\mu\text{m}$ , respectively. In order to increase the accuracy of the experimental data, the probe beam was adjusted near the center of the pump beam. The samples were chromium films with a thickness of 145 nm on glass substrate. The analyzer was put in front of the detector to suppress the stray ray from the pump beam. In order to improve the signal-to-noise ratio (SNR), the pump beam was chopped at 1 kHz by a chopper. The reflectivity signal of the probe beam was monitored by a digital signal processing (DSP) lock-in amplifier (Stanford Research Systems, SR830). The lock-in amplifier was connected to a computer by a data acquisition card. Pump-probe technique was used to measure the time-resolved reflectivity. The time interval and total acquisition time of each data acquisition were 1 ms and 2 s, respectively. So each experimental data point in Fig. 2 is an average value of 2000 data.

The experiments were carried out under atmospheric pressure. The chromium film were

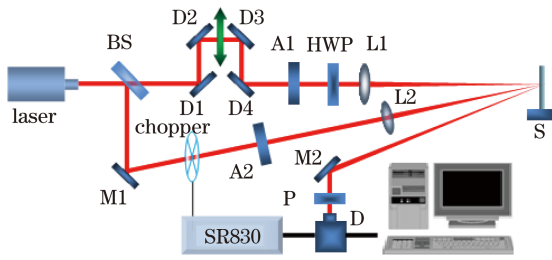


Fig. 1. Experimental setup for measurement of the femtosecond time-resolved reflectivity. The parameters of the femtosecond laser are 8 nJ/pulse, 800 nm, 76 MHz, and 70 fs. BS: beam splitter; D1–D4: delay lines; M1, M2: mirrors; A1, A2: attenuators; HWP: 1/2 wave plate; L1, L2: convergent lenses; S: chromium film; P: polarization plate; D: detector; SR830: lock-in amplifier.

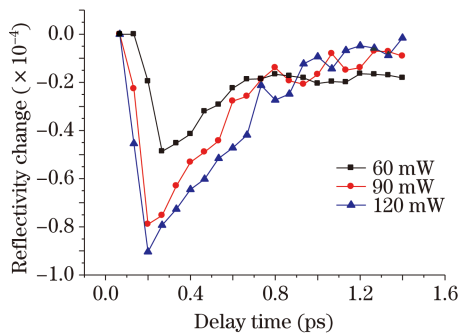


Fig. 2. Experimental results of time-resolved relative reflectivity for three different pump powers.

cleaned with acetone and ethanol under illumination of yellow light. The temperature of this experiment was around 300 K. The fluctuation of the femtosecond laser was about 1%. Figure 2 shows the experimental results of relative reflectivity changes as a function of delay time for three different pump powers of 60, 90, and 120 mW, respectively.

As shown in Fig. 2, the amount of reflectivity change increases with the power of the pump laser. The largest reflectivity change for 120 mW is observed among the three different pump powers. The transient relative reflectivity change might be due to the redistribution of unoccupied electronic states near the Fermi energy level for chromium<sup>[3,11]</sup>. The decrease in reflectivity results from the fact that more electrons absorb the probe beam. Since the electron temperature increases with the power of the pump beam and more movement of excited electrons appears for the larger pump power, the reflectivity change increases with the pump power.

Figure 2 also shows that the reflectivity change process consists of three different time stages. Firstly, the transient relative reflectivity decreases rapidly for the delay time up to 200 fs and reaches the minimum point at around 200 fs. Secondly, the increasing reflectivity occurs for the delay time of 200–900 fs. Thirdly, the reflectivity after delay time of 900 fs rises little to near a constant. Two major processes of electron-electron collision and scattering process and electron-phonon coupling process occur in the interaction between the femtosecond laser and the chromium film. Supposing that the electron and phonon systems are regarded as two thermal subsystems, the reflectivity change process might be explained by the TTM.

When the chromium film is irradiated by the femtosecond laser, the pump laser pulse delivers energy to the electrons which thermalize rapidly via electron-electron collision and scattering. Thermal turbulence of the chromium film is induced by the pump beam. Because the femtosecond laser pulse is shorter than the electron-phonon coupling time, this experiment can resolve the nonequilibrium electron-phonon temperature difference. The electrons can be heated up to a high temperature at first, and then cool down by electron-phonon coupling process. The space and time evolution of the electron temperatures  $T_e$  and lattice temperatures  $T_l$  can be modeled by a pair of coupled nonlinear differential equations<sup>[18]</sup>,

$$C_e(T_e) \frac{\partial T_e}{\partial t} = K \nabla^2 T_e - G(T_e - T_l) + P(z, t), \quad (1)$$

$$C_l \frac{\partial T_l}{\partial t} = G(T_e - T_l), \quad (2)$$

where the energy source term  $P(z, t)$  can be described by<sup>[19]</sup>

$$P(z, t) = 0.94 \frac{1-R}{t_p \mu} S \exp\left[-\frac{z}{\mu} - 4 \ln 2 \left(\frac{t}{t_p}\right)^2\right], \quad (3)$$

where  $R = 0.25$  is the reflectivity of chromium film,  $t_p$  is the FWHM of the femtosecond laser,  $\mu$  is the penetration depth,  $S$  represents the incident energy,  $z$  is the depth coordinate of chromium film,  $C_l$  and  $C_e$  are the lattice and electron heat capacities, respectively,  $K$  is the thermal conductivity of the electrons,  $G$  denotes the electron-phonon coupling constant.

The temperature change process of the electron and phonon can be described by numerical simulation with Eqs. (1)–(3). Using chromium film as an example, the electronic heat capacity is proportional to its temperature  $C_e = \gamma T_e$ ,  $\gamma = 194 \text{ J}/(\text{m}^3 \cdot \text{K}^2)$ ,  $C_l = 3.6 \times 10^6 \text{ J}/(\text{m}^3 \cdot \text{K})$ , with the electron-phonon coupling constant  $G = 4.2 \times 10^{17} \text{ W}/(\text{m}^3 \cdot \text{K})$ . Because the pulse width of the femtosecond laser is shorter than the conduction process of the electron, the term  $K \nabla^2 T$  can be neglected<sup>[20]</sup>.

Numerical simulations of the changes of electron temperature and phonon temperature versus time delay between the probe and the pump beams are shown in Figs. 3 and 4, respectively. Because the heat capacity of the electrons is small, the electron temperature increases rapidly and reaches the maximum value after the chromium film is irradiated by the pump beam. Figure 3 shows that the rising time of the electron temperature is about 100–200 fs. The electron-electron collision and scattering process plays a key role in the process of the rising electron temperature. The sharp rising stage of the electron temperature could result in the decrease of reflectivity in Fig. 2. Then the electron temperature drops slowly through electron-phonon coupling process, as shown in Fig. 4. Correspondingly, the reflectivity increases slowly after the electron-phonon interaction, as shown in Fig. 2. So the process of the increment in reflectivity can be explained with the electron-phonon coupling process.

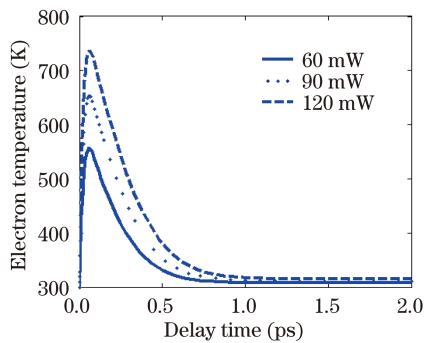


Fig. 3. Electron temperature evolution for three different pump powers.

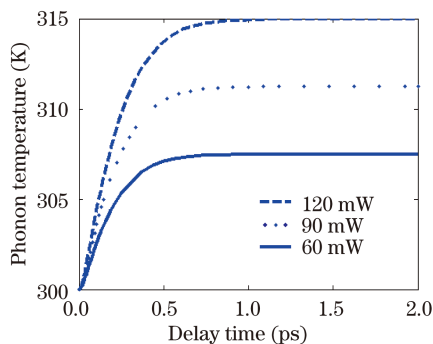


Fig. 4. Phonon temperature evolution for three different pump powers.

The fast decrease of the reflectivity is about 0–200 fs and the slower recovery of the reflectivity is in the 200–900 fs time range. In comparison, we find that the fast decrease of the reflectivity is about 0–100 fs and the slower recovery of the reflectivity is in the 100–600 fs time range in Ref. [16]. We note that the reflection and transmission coefficients of sample are  $R = 0.46$  and  $T = 0.16$  in Ref. [16]. However, the reflection and transmission coefficients of chromium film are  $R = 0.25$  and  $T = 0.12$  in our experiment. These different values might be due to the different thicknesses and densities of chromium films on the glass substrate which were made with different production technologies. These different values of  $R$  and  $T$  play an important role in the measurement of the relative reflectivity change. The reflectivity rises little after the delay time of about 900 fs for reaching the thermal equilibrium between electron and phonon temperature. In this experimental setup, the slight alignment error of the delay line might be the reason for the small fluctuation after 900 fs. The optical spot of the probe beam might slightly fluctuate around the center of the optical spot of the pump beam in the moving process of delay line. The slight change of the relative position affects directly the experimental results.

We also note that the reflectivity changes are different for three different pump powers after the delay time of 900 fs for reaching the thermal equilibrium. This phenomenon can be attributed to different equilibrium temperatures in Fig. 4. We conclude that the relative time-resolved reflectivity can be explained with the interaction between the electrons and phonons. Considering that the chromium mask is widely used in microelectronic industry, this result might be helpful for further study of ultrafast electron dynamics of chromium mask in micro- and nano-scale.

In summary, the transient time-resolved reflectivity of the chromium film is investigated by femtosecond time-resolved pump-probe technique. Experiments are performed for three different pump powers. Experimental results show that the reflectivity change increases with the power of the pump laser. The ultrafast dynamics of electrons are influenced by the electron-electron collision and the electron-phonon coupling interaction. The sharp decrease of the reflectivity is mainly due to the electron-electron interaction in the 0–200 fs time range. Subsequently, the electron-phonon coupling process plays an important role in the recovery of reflectivity in the 200–900 fs time range. The reflectivity comes to a near-constant value after 900 fs, indicating that a thermal equilibrium is reached. Comparison of the experimental results with numerical simulation of the TTM is given. The experimental results can be explained properly. It is helpful for understanding of the electron ultrafast dynamics in chromium films.

This work was supported by the National Natural Science Foundation of China (No. 60878035), the Shanghai Science and Technology Committee (No. 07SA14), and the National “973” Program of China (No. 2006CB806000).

## References

1. L. D. Pietanza, G. Colonna, S. Longo, and M. Capitelli, *Thin Solid Films* **453**, 506 (2004).
2. J. Hohlfeld, D. Grosenick, U. Conrad, and E. Matthias, *Appl. Phys. A* **60**, 137 (1995).
3. G. L. Eesley, *Phys. Rev. Lett.* **51**, 2140 (1983).
4. G. L. Eesley, *Phys. Rev. B* **33**, 2144 (1986).
5. A. Bartels, F. Hudert, C. Janke, T. Dekorsy, and K. Köhler, *Appl. Phys. Lett.* **88**, 041117 (2006).
6. H. E. Elsayed-Ali and J. W. Herman, *Appl. Phys. Lett.* **57**, 1508 (1990).
7. J. Hohlfeld, S.-S. Wellershoff, J. Güdde, U. Conrad, V. Jähnke, and E. Matthias, *Chem. Phys.* **251**, 237 (2000).
8. N. Del Fatti, R. Bouffanais, F. Vallée, and C. Flytzanis, *Phys. Rev. Lett.* **81**, 922 (1998).
9. S. D. Brorson, J. G. Fujimoto, and E. P. Ippen, *Phys. Rev. Lett.* **59**, 1962 (1987).
10. R. W. Schoenlein, W. Z. Lin, J. G. Fujimoto, and G. L. Eesley, *Phys. Rev. Lett.* **58**, 1680 (1987).
11. H. E. Elsayed-Ali, T. B. Norris, M. A. Pessot, and G. A. Mourou, *Phys. Rev. Lett.* **58**, 1212 (1987).
12. J. Hohlfeld, J. G. Müller, S.-S. Wellershoff, and E. Matthias, *Appl. Phys. B* **64**, 387 (1997).
13. Z. Han, C. Zhou, E. Dai, and J. Xie, *Opt. Commun.* **281**, 4723 (2008).
14. Z. Han, C. Zhou, E. Dai, and J. Xie, *Chinese J. Lasers (in Chinese)* **35**, 768 (2008).
15. J. Xie, C. Zhou, E. Dai, and Z. Han, *Opt. Commun.* **281**, 5396 (2008).
16. H. Hirori, T. Tachizaki, O. Matsuda, and O. B. Wright, *Phys. Rev. B* **68**, 113102 (2003).
17. E. Dai, C. Zhou, and G. Li, *Opt. Express* **13**, 6145 (2005).
18. S. I. Anisimov, B. L. Kapeliovich, and T. L. Perelman, *Sov. Phys. JETP* **39**, 375 (1975).
19. J. Kim and S. Na, *Opt. Laser Technol.* **39**, 1443 (2007).
20. B. N. Chichkov, C. Momma, S. Nolte, F. von Alvensleben, and A. Tünnermann, *Appl. Phys. A* **63**, 109 (1996).